Mol. Cryst. Liq. Cryst., Vol. 320, pp. 77–88
Reprints available directly from the publisher
Photocopying permitted by license only

Published by license under
the Gordon and Breach Science
Publishers imprint.
Printed in Malaysia.

Photocontrol of Smectic Spacing

W.R. FOLKS[1,#]S. KEAST[1], T. A. KRENTZEL[#], B. ZALAR[#],
H. ZENG[#], YU. A. REZNIKOV[1], M. NEUBERT[1], S. KUMAR[1,#],
D. FINOTELLO[1,#], and O. D. LAVRENTOVICH[1,*]
[1]Liquid Crystal Institute, [#]Department of Physics, and [*]Chemical Physics
Program, Kent State University, Kent, OH, 44242

We report on the results of optical, X-ray and NMR studies of light-induced phenomena in smectic phases triggered by molecular phototransformations. UV irradiation causes trans-to-cis isomerization of the dopant molecules while irradiation in the visible part of the spectrum facilitates cis-to-trans relaxation. Cis-to-trans isomerization decreases the smectic layers' spacing; as the result, a smectic slab undergoes an undulation instability and/or formation of focal conic domains. These textures are nonuniform and scatter light; this effect can be used for optical data storage. The opposite trans-to-cis isomerization disorders the orientation of molecules and increases the thickness of smectic layers. Two beams of different wavelengths with distinct yields of isomerisation can be used to write and erase optical information.

Keywords: photoisomerization; smectic phases; undulations; trans-cis isomerization

INTRODUCTION

Light-induced Frederiks effect [1] and surface photoalignment [2] are two spectacular manifestations of the high sensitivity of the nematic phase to light irradiation. In contrast, smectic (Sm) materials should be less sensitive, since Frederiks and surface- driven instabilities are hindered by their layered structure. Usually, the light-induced effects in smectic materials are caused by indirect thermal mechanisms. For example, in the thermo-optic effect discovered by Kahn [3], a high-intensity laser beam is used to heat a smectic A (SmA) cell; when the light intensity is sharply reduced, the smectic layers tend to contract as the sample cools down. If the thickness of the whole smectic slab remains fixed, this contraction results in undulations and formation of focal conic domains. Recently, a number of results have been reported on optical switching in the chiral smectic C (SmC*) phase caused by polarization changes [4,5] or by photochemically induced phase transitions [5-7].

In this work, we summarize the features of a method that allows for a direct optical control of smectic layers' spacing. It is based on phototransformation of dopant molecules such as azobenzene and its derivatives. A typical system in our study study was a mixture of octylcyanobiphenyl (8CB) and diheptylazobenzene (7AB), molar ratio 90.4:9.6, phase diagram $\left(<24^0\mathrm{C}\right)\mathrm{Sm\,A}\left(36^0\mathrm{C}\right)\mathrm{N}$. Mixtures of other thermotropic smectic materials with other photosensitive materials (such as azobenzene) give similar results provided the photosensitive material is capable of trans-to-cis and cis-to-trans light-induced isomerization.

Azobenzene and its derivatives such as 7AB exist in two isomer forms, trans and cis. The elongated trans-isomer is the ground state of the molecule. Upon UV illumination the molecules convert into a strongly bent metastable cis-form. The latter can be returned into the trans-form thermally or by illumination with longer wavelength (normally above 420 nm). The length of the trans-7AB molecule is close to the SmA layer spacing of 8CB ($\approx 32\,\AA$) and is thus easy to incorporate into the 8CB smectic layers; in fact, 7AB is a mesomorphic material by itself. The cis-isomers are strongly bent and thus less symmetric, Fig.1. In addition, to study light-induced instabilities in the SmC* phase we prepared a mixture of a ferroelectric SmC* material ZLI-3774 (EM Industries, phase diagram $(<-30)\mathrm{Sm\,C}^*(62)\mathrm{SmA}\left(76^0\mathrm{C}\right)\mathrm{N}$) and 7AB(12% in weight).

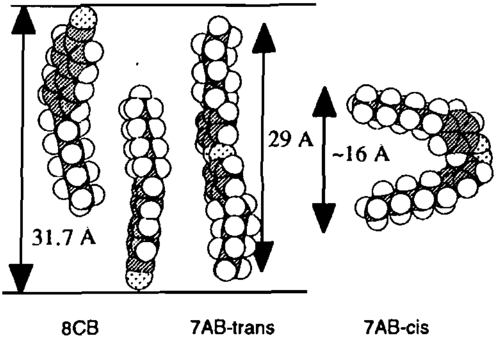

Fig.1. Trans-isomers of 7AB closely match the layer spacing in the SmA phase of 8CB host. In contrast, highly bent cis-isomers are difficult to incorporate into the smectic layers.

LIGHT-INDUCED LAYER UNDULATIONS AND FOCAL CONIC DOMAINS

The radiation from a single transverse mode of He-Ne laser ($\lambda = 632.8$ nm, power 10 mW, beam divergence 1.2 mrad) was directed normally to the flat cell with smectic material confined between two glass plates (separated by distances $h = 15 - 180$ μm). The plates were treated for an appropriate orientation of liquid crystal director (homeotropic or planar, as discussed below). The nonscattering (directly passing through the cell) light was cut off by a small screen. If the smectic layers are parallel to the bounding glass plates (homeotropic orientation of the molecules), the illuminated spot produces a strongly scattering texture formed by parabolic focal conic domains (PFCD's), Fig.2 [8,9]. The axes of symmetry of the parabolas are normal to the cell's plane. The periodicity P of the PFCD's increases with h, closely following the relation $P \sim \sqrt{h}$. In cells with molecules parallel to the plates (these cells were initially aligned in a strong magnetic field), the He-Ne light causes PFCD's with axes in the plane of the cell, Fig.3. This process is similar to the appearance of PFCD's in smectic cells when 8CB is cooled down and forms a chevron structure [10]. The phenomenon was more pronounced if the samples were preliminary illuminated with UV light.

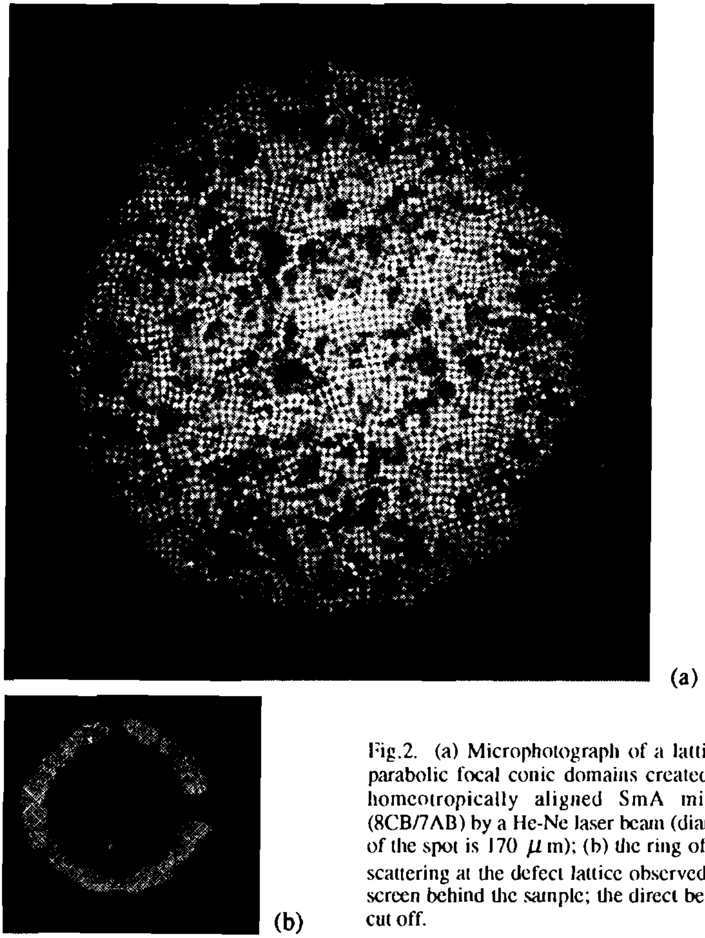

Fig.2. (a) Microphotograph of a lattice of parabolic focal conic domains created in a homeotropically aligned SmA mixture (8CB/7AB) by a He-Ne laser beam (diameter of the spot is 170 μm); (b) the ring of light scattering at the defect lattice observed on a screen behind the sample; the direct beam is cut off.

The silent time t_s of instability (i.e., the time interval between the beginning of irradiation and the appearance of the scattering structure) decreases from ~ 100 sec at $I_{in} = 0.2\,\mathrm{W/cm^2}$ to ~ 1 sec at $I_{in} = 1.3\,\mathrm{W/cm^2}$ and follows the rule $t_s \sim 1/\left(I_{in} - I_{in}^{thr}\right)$, where $I_{in}^{thr} = 0.1\,\mathrm{W/cm^2}$ is the threshold intensity. No instability was detected when $I_{in} < I_{in}^{thr}$.

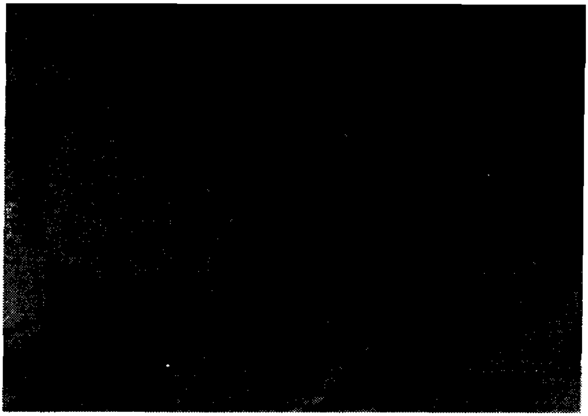

Fig.3. Microphotograph of a parabolic focal conic domains created in a planar sample of the SmA mixture 8CB/7AB by a He-Ne laser beam.

Once the He-Ne beam is cut off, the pattern gradually fades after ~ 1 – 10 min. The opto-optical effect becomes weak after several cycles of He-Ne laser switching on-off. The ability of the system to respond to the He-Ne laser beam is restored by UV illumination which causes trans-cis transformations. An opposite effect occurs when the cell is held at a high temperature in the dark and the cis-isomers are converted into the stable trans-form. When the cell is cooled down to room temperature to restore the homeotropic SmA texture, the He-Ne illumination has no effect. Also, no effect occurs in cells containing pure 8CB.

The efficiency of the instability in the mixture 8CB:7AB strongly depends on λ. First, a higher $\lambda = 710$nm leads to a weaker effect with a threshold larger than that in the He-Ne case. For $\lambda = 750$ and $\lambda = 830$nm, no instability was observed. The efficiency also decreases when λ decreases: $\lambda = 510$, 488, 460, and 440 nm yield no effect. Instead, the short-wavelength illumination causes either melting of the SmA phase, or, indirectly produces the scattering textures when the beam is cut off and the sample cools down; this effect is caused by thermal contraction of the layers under cooling. Moreover, an Ar laser beam, $\lambda = 488$ nm (or UV light as well) supresses the instability created by the He-Ne beam.

The SmC* material ZLI-3774 doped with 7AB, was placed between lecithin-treated glass plates separated by a distance 51.0 μm. At temperatures above $65^o C$ the mixture is in the SmA phase. For the 8CB/7AB mixture, the He-Ne illumination creates a PFCD texture. The instability also occurs at room temperature in the SmC* phase. However, the qualitative features of the SmC* instability are different from those of the SmA one: in SmC*, there are two light-scattering rings rather than one. The larger outer ring appears first and corresponds to an undulation periodicity $P = 1.2 \pm 0.2\,\mu m$. As it gradually decays with time, a smaller ring begins to develop. The smaller ring corresponds to a periodicity $P = 5.1 \pm 0.2\,\mu m$ and its appearance on the screen is basically identical to the light scattering patterns of PFCD's observed for the SmA phase. Microscopic observation reveals that the illuminated area has the textural characteristics of a PFCD lattice. This PFCD's lattice in the SmC* cell is apparently preceded by a true undulation instability.

It is well known that undulation and PFCD patterns in Sm cells with fixed thickness occur when the smectic layers are contracted [11]. The critical fraction Δd of the layer spacing d sufficient to produce undulations is $\Delta d = 2\pi d\Lambda / h$, where $\Lambda = \sqrt{K/B} \sim d$, K being the splay elastic constant and B the compressibility modulus. The PFCD instability occurs at a slightly higher threshold (by a factor of 1.7) [12]. Each PFCD is formed by layers folded around two singular parabolas, Fig.4.

The physical reason of the appearance of the PFCD as a response to contracted layers is the multiconnectivity of the smectic layers in PFCD's. To demonstrate this, let us consider the function $u(x, y, z_0)$ introduced by Rosenblatt et al. [13] to describe the displacement of layers along the vertical axis z. Each point (x, y) that belongs to a layer originally forming a plane $z = z_0$, shifts by a distance u along z when the PFCD forms. The axis z is normal to the initial layers; $z=0$ is located in the center of the cell. At points $(x = 0, y = 0)$ all layers remain normal to the z-axis and $u(0,0,z_0)$ shows where the layer crosses the z-axis. The equation for $u(x, y, z_0)$ reduces to $(u+f)^3 - (u+f)^2(3f - 2z_0) + 2f(u+f)(f - 2z_0) = 0$, with f being the focal length of the parabolas. The last cubic equation has three real roots

$\left(z_1 = f + z_0; z_2 = -z_0; z_3 = -f + z_0\right)$ when $-f/2 < z_0 < f/2$, and, one real root when $-h/2 < z_0 < -f/2$ or $f/2 < z_0 < h/2$. Thus, each layer located initially between the points $(-f/2, f/2)$, transforms into a triple-connected layer when the PFCD forms. Such a layer crosses the z-axis three times and its effective "thickness" is $3d$. This explains why the PFCD's occur upon contraction of the layers: multiple connected layers allow the system to fill the space between the plates by thinner layers without changing the total number N of these layers, i.e. without nucleation and propagation of dislocations.

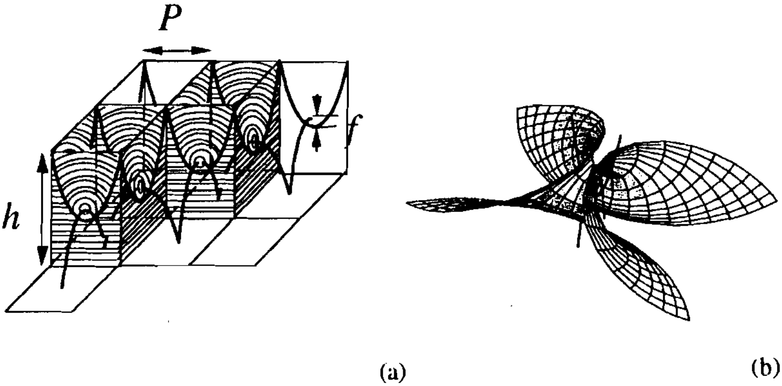

Fig. 4. Layer and defect configurations in parabolic focal conic domains: (a) periodic lattice corresponding to the texture of Fig.2a; thick lines represent parabolas; thin lines are cross-sections of the smectic layers; (b) in the center of the parabolic focal conic domain, the smectic layers are multiconnected and cross any vertical axis three times.

Using the idea that the total number of layers remains constant, $N = h/d = (h-2f)/(d+\Delta d) = const$, one finds that the formation of PFCD's accommodates the change in the layers' spacing by $\Delta d = -2fd/h$. Since the distance P between the ends of the parabolas is $P = 2\sqrt{2fh}$, one gets an estimate of the layer's contraction through the parameters P and h which are easily determined experimentally: $-\Delta d/d = P^2/4h^2$. For typical P and h, $P/h \sim 0.1$, the photo-induced contraction of each layer is of the order of $0.1\AA$. This estimate can be compared to actual in-situ measurements of the layer spacing of SmA layers discussed in the next section.

IN-SITU X-RAY MEASUREMENTS OF LIGHT-CONTROLLED SMECTIC LAYER SPACING [14].

X-ray measurements were carried out using a Rigaku 18kW rotating anode source with a pair of Ge(111) single crystals as monochromator and analyzer. The sample was aligned to obtain a planar molecular orientation. To investigate the dynamics of light-induced instabilities in the SmA 8CB/7AB mixture, we measured the smectic spacing while irradiating the sample with non-polarized UV light (366 nm) followed by either: (a) relaxation with no illumination, or (b) exposure to He-Ne laser light. The results in Fig. 5 clearly demonstrate that the layer's spacing is controlled by the light. UV light significantly increases the layer spacing, while the red He-Ne illumination enhances the layers' contraction. The light-induced changes are significant, about $0.15\,\AA$ at $24^{\circ}C$ and even larger at higher temperatures.

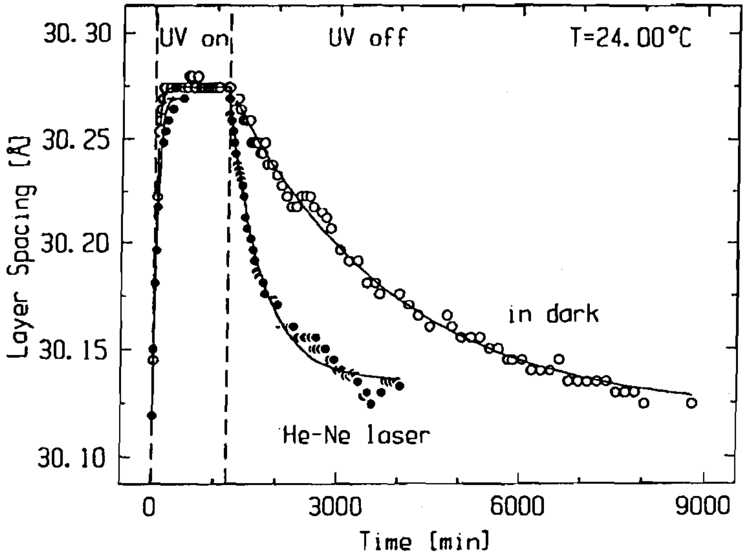

Fig.5. Evolution of the SmA layers spacing under UV illumination and a consequent realization with UV light off (in dark) open circles. Closed circles: in addition to UV, a He-Ne laser beam illuminates the sample; the He-Ne illumination continued after the UV was turned off.

Obviously, there are at least two effects of light illumination on Sm samples: heating and molecular phototransformations. The temperature dependence of the layer spacing for pure 8CB and the mixture 8CB/7AB is shown in Fig. 6. Note that an increase of the layers' thickness by 0.15 *Å* requires heating the sample by about $10°C$; this temperature increase is unlikely under UV illumination (the sample was thermostabilized at the level of $\pm 1\, mK$). In any case, the thermal- and photo- mechanisms work in opposite directions for the red light: according to Fig. 6, the temperature raise would increase the layer spacing, while according to Fig. 5, the He-Ne illumination facilitates layers' contraction.

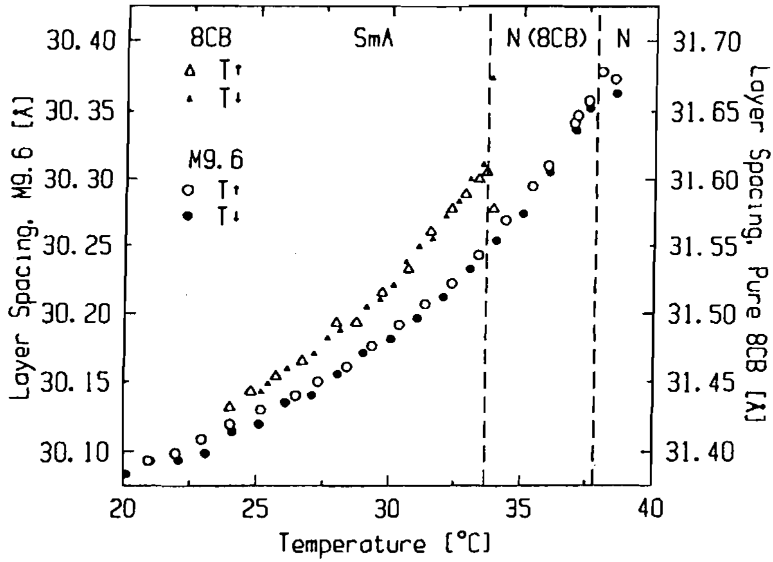

Fig.6. Temperature dependencies of the smectic layer spacing in pure 8CB and in the 8CB/7AB mixture.

X-ray data help to understand why the efficiency of the light-induced phenomena is highest when the sample is preliminary exposed to UV light: the latter creates an excess of cis-isomers and the relative contraction of layers by visible light is larger. The concentration of cis-isomers at the photostationary state strongly depends on the wavelength of light. It is relatively high (40-80%) in the UV region, decreasing drastically to about

10% or less when the wavelength becomes larger, above 400 nm. The dependence of the cis-concentration on the light wavelength in the visible range allows one to realize different cycles of writing-erasing information in a smectic cell. For example, the appearance and disappearance of the scattering structures is achieved when the sample is illuminated with alternating Ar (488 nm) and He-Ne (633 nm) beams.

ORDER PARAMETER

NMR studies were performed to verify the nature of molecular rearrangements under light illumination. Two complementary 8CB/7AB mixtures were prepared: one with deuterated host 8CB and one with deuterated guest 7AB. The samples were illuminated with UV light.

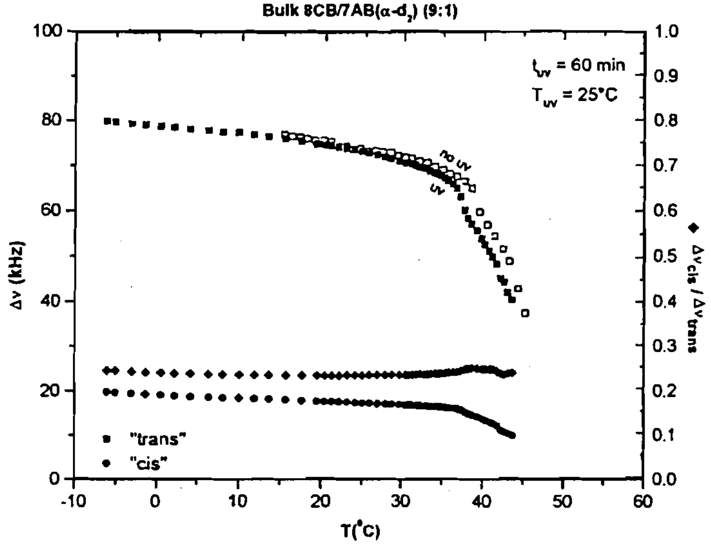

Fig.7. Splitting of the NMR lines as a function of temperature for 8CB/7AB mixture with a deuterated 7AB. The sample was illuminated at 25 °C for 60 min and then placed in the NMR spectrometer.

Figure 7 shows the typical behavior of the nematic order parameter (proportional to the splitting $\Delta\nu$ in the NMR quadrupolar resonance line [15]) of the deuterated 7AB component. UV irradiation decreases the order, while relaxation from cis-to-trans state restores higher values of the order parameter. Analysis of the NMR spectral patterns [16] also indicates that the cis isomers preserve a uniaxial character of ordering with their symmetry axis matching that of the nematic and smectic A phases. The increase in the layer spacing under UV illumination can be understood as a disorientation of the smectic A matrix by highly bent cis molecules; these isomers decrease the scalar order parameter and increase the layer spacing. In contrast, the elongated trans-isomers enhance the order and decrease the spacing; the latter results in layer undulations and formation of focal conic domains.

SUMMARY

We described the structural aspects of the opto-optical effect caused by low-power He-Ne laser irradiation in SmA and SmC liquid crystals doped with photosensitive molecules capable of trans-cis isomerization. The effect manifests itself in the appearance of a scattering lattice of parabolic focal conic domains or undulated layers, under light illumination that facilitates cis-to-trans isomerizarion. With dopant diheptylazobenzene the instability is pronounced in the region $600 < \lambda < 750$ nm. UV-irradiation increases the concentration of cis-isomers and expands the smectic layers, while visible light accelerates the cis-to-trans relaxation and decreases the spacing. The changes in the layer spacing are accompanied by the changes in the orientational order parameter: cis-isomers created under UV illumination disorient the material; their relaxation back to the trans-state enhances the order.

Acknowledgments

This research was supported by the NSF ALCOM Center, Grant No. DMR89-20147.

References

[1.] I.C. Khoo and S.-T. Wu, *Optics and Nonlinear Optics of Liquid Crystals* (World Scientific, Singapore, 1993).

[2.] K. Ichimura, Supramolecular Science **3**, 67 (1996); and references therein.

[3.] F. J. Kahn, Appl. Phys. Lett. **22**, 111 (1973).

[4.] T. Ikeda, T. Sasaki, and K. Ichimura, Nature 361, 428 (1993).

[5.] H.G. Walton, H.J. Coles, D. Guillon, and G. Poeti, Liq. Cryst. **16**, 333 (1994).

[6.] M. Negishi, K. Kanie, T. Ikeda, and T. Hiyama, Chem. Lett. 583 (1996).

[7.] K. Shirota and I. Yamaguchi, Jpn. J. Appl. Phys. **36**, L1035 (1997).

[8.] W.R. Folks, Yu.A. Reznikov, L. Chen, A.I. Khizhnyak, and O.D. Lavrentovich, Mol. Cryst. Liq. Cryst. **261**, 259 (1995).

[9.] W.R. Folks, Yu.A. Reznikov, S.N. Yarmolenko, and O.D. Lavrentovich, Mol. Cryst. Liq. Cryst. **292**, 183 (1997).

[10.] Y. Ouchi, Y. Takanishi, H. Takezoe, and A. Fukuda, Jpn. J. Appl. Phys. **28**, 2547 (1989).

[11.] P.G. de Gennes and J. Prost, *The Physics of Liquid Crystals* (Clarendon Press, Oxford, 1993).

[12.] N. A. Clark and A. J. Hurd, J. Phys. (Paris) **43**, 1159 (1982).

[13.] C. Rosenblatt, R. Pindak, N. A. Clark and R. B. Meyer, J. Phys. (Paris) **38**, 1105 (1977).

[14.] T.A. Krentsel (Lobko), O.D. Lavrentovich, and S. Kumar, Mol. Cryst. Liq. Cryst. **304**, 463 (1997).

[15.] A. Abragam, *The Principles of Nuclear Magnetism* (Clarendon, Oxford, 1962).

[16.] B. Zalar *et al.*, to be published.